Geochemistry of Banded Iron Formations and their host rocks from the Central Eastern Desert of Egypt: A working genetic model and tectonic implications.

V43F-0179: Hydrothermal Systems in Oceanic Arcs III

EL-SHAZLY, Aley K.[1], **KHALIL, Khalil Isaac**[2] , **and HELBA, Hossam H.**[2]

(1) Geology Department, Marshall University, Huntington, WV 25755

(2) Geology Department, Faculty of Science, Alexandria University, Egypt

Sponsored by NSF-OISE-1004021

Abstract

Thirteen banded iron formations (BIF) occur intercalated with Neoproterozoic volcano-sedimentary units in the Egyptian Central Eastern Desert (CED). These BIFs consist of layers of magnetite and hematite alternating with quartz-rich layers containing garnet, epidote, ± calcite in the southern parts of CED, and chlorite ± stilpnomelane, and calcite in the north. Localized hydrothermal alteration manifested by secondary Ca–bearing minerals affected all BIFs. All BIFs and their host rocks were strongly deformed and metamorphosed under greenschist to epidote amphibolite facies conditions during the collisional stage of the Pan African orogeny.

Geochemically, CED BIFs have higher Fe/Si compared to Algoma, Superior, or Rapitan BIF types. All BIFs have rare earth element – Y patterns similar to modern day oceanic water, with a few samples displaying a weak positive Eu anomaly. All BIFs have high SiO_2/Al_2O_3 and Fe/Ti, and low Al/(Al+Fe+Mn), which suggest a hydrogenous origin with hydrothermal contributions and minor detrital component. Geochemical trends, Ho/Y, and Pr/Yb values suggest deposition of Wadi El Dabbah BIF closest to land and Um Nar and Wadi Kareim closest to hydrothermal vents. Host metavolcanic and metavolcaniclastic rocks show chemical signatures indicative of an immature oceanic arc setting with MORB affinities for the southern bodies and back- or fore- arc basin affinities for the northern localities. These results lead to the conclusion that CED BIFs and their host rocks formed in small sloped or terraced silled basins in the back- and fore-arc areas surrounding an immature island arc. Restricted circulation of hydrothermal fluids in these basins concomitant with arc volcanism increased Fe^{+2} and Si in solution. During periods of arc quiescence, oxidation of Fe^{2+} led to deposition of Fe-oxyhydroxide. Diagenesis formed fine-grained magnetite, whereas subsequent hydrothermal alteration and metamorphism formed porphyroblastic magnetite and specularite.

I- Introduction

- The common occurrence of BIFs in Archean and Paleoproterozoic terranes versus their paucity in Neoproterozoic or younger sequences is typically used to constrain the GOE at 2.5 Ga.
- BIFs occur intercalated with Neoproterozoic volcaniclastic rocks in 13 localities in the Egyptian CED (Fig. 1). These small deposits have been classified as Algoma type BIF.
- Most BIFs are characterized by Fe^T contents that are higher than average Algoma or Superior BIFs (44 vs. 28 Fe^T wt%).
- Ali et al. (2010) and Stern et al. (2013) attributed BIF deposition in CED to concomitant melting of glacial ice c. 750 Ma, whereas other authors suggested origins ranging from metasomatic to volcanogenic for select deposits (e.g. Salem et al., 1994; El Habaak, 2004; Basta et al., 2011; El-Shazly and Khalil, 2016).
- This study focuses on 8 of the 13 deposits and aims at understanding the origin of the CED BIFs in the context of the tectonic evolution of the area, and the effects of hydrothermal alteration/ weathering on their Fe^T.

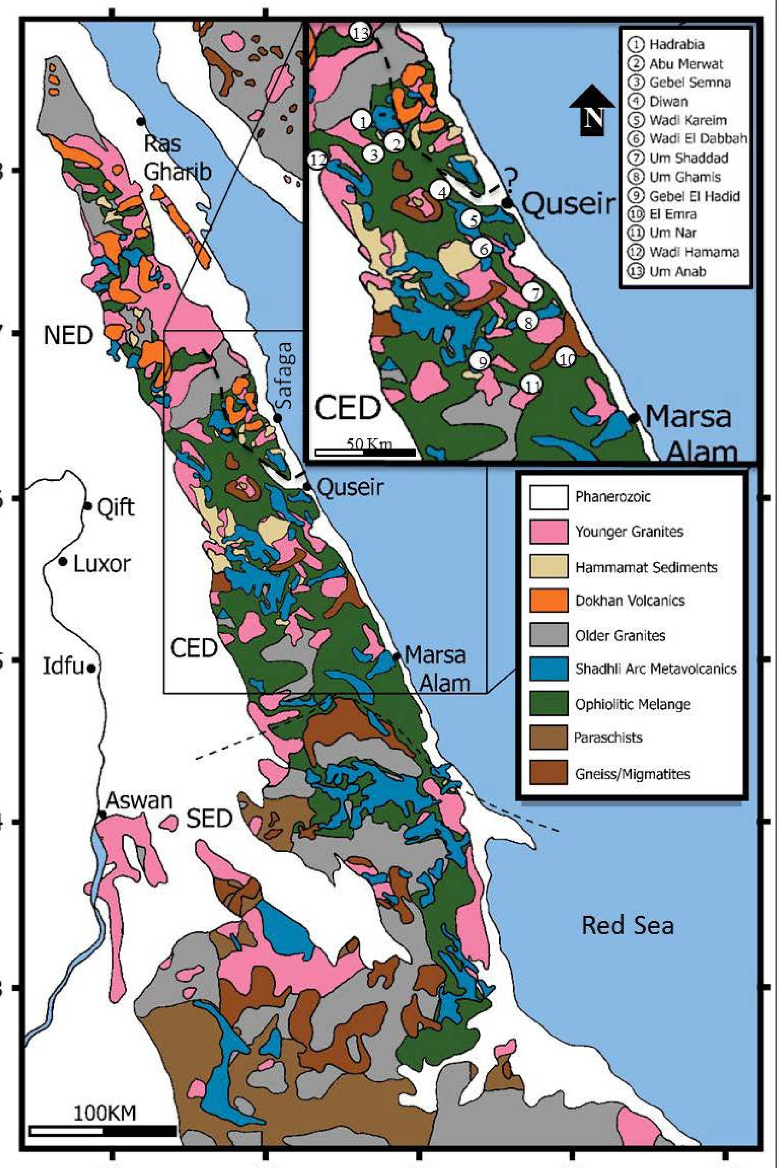

Fig. 1: Simplified Geologic map of Egypt showing the locations of 13 BIFs

II- Geologic Setting

- The Eastern Desert of Egypt exposes Precambrian basement rocks that consist of: (i) "metamorphic core complexes" consisting of 1.8 Ga – 680 Ma migmatites and gneisses (ii) 850–700 Ma "ophiolitic mélanges" and coeval "arc assemblages" that include volcaniclastic and volcanic rocks intercalated with epiclastic sedimentary rocks; (iii) "Older granitoids" intruded 710–610 Ma; (iv) 630–592 Ma old, high- K, calcalkalic Dokhan arc volcanic rocks, and 606–585 Ma old Hammamat molasse type sedimentary rocks that overlie units (i)–(iii); and (v) "Younger granitoids" intruded < 620 Ma (Fig. 2).
- The NED is characterized by a paucity of serpentinites, abundance of post- orogenic "Younger granitoids", and Dokhan volcanics. The CED is predominated by ophiolitic mélanges + arc assemblages ± banded iron formations. The SED is characterized by the predominance of "Older granitoids" + gneisses and migmatites (Fig. 1).
- BIFs and their host rocks belong to the "island arc" and "ophiolitic mélange" units (Figs. 1 & 2). Both rock types were regionally metamorphosed under greenschist to epidote amphibolite facies conditions.
- Metamorphic conditions range from 520 ± 30°C, 5 ± 2 kbar for Um Nar in the south to 400 ± 50°C, 4 ± 2 kbar four Abu Marwat in the north.
- The southern areas of Um Nar–Wadi El Dabbah are characterized by NE to E- verging folds (Fig. 3a), whereas the northern areas of Abu Marwat – Wadi Kareim show SW-directed folds and thrusts.
- The BIF layers are a few cm to 15 m thick and are interlayered with metavolcaniclastics (Fig. 3a & b).
- Most CED BIFs are femicrites with rhythmic banding defined by iron oxide rich layers alternating with jaspilites (Fig. 3c and d).
- Lithic fragments in BIF layers are rare in most deposits, but quite common in W. El Dabbah (Fig. 3d).

II- Geologic Setting (continued)

- The deposits of Hadrabia and Abu Marwat have layers with a distinct pisolitic texture (Fig. 3e-f).
- All deposits show some evidence of localized hydrothermal alteration manifested by veins of calcite and other Ca–rich minerals (Fig. 3g), and/ or a characteristic porous texture (Fig. 3h).

Age (Ma)	Continent/ Arc SED	Inter-Arc Basin CED	Continent/Arc CED & NED	Deformation/ Other
<570			Younger Granite	
606 — 585			Contact metam-orphism; Hammamat; Dokhan Volcanism	D4b: Najd system: sinistral
620 — 580				D4a: Najd system: dextral
614 — 590			Pan-African Orogeny; Partial exhumation of core complexes	D3: transpression/ lateral extrusion ; N and S directed thrusting
640 – 616			Regional metamorph-ism Older Syntectonic Granites and Gabbros	Island arc accretion
680 – 640			Obduction, accretion, and basin closure	D2: N-directed thrusting and folding
690 – 670			Older granite (El-Imra)	
850 — 700	Younger (Shadhli) metavolcanics Shiatian granitoids?	Volcaniclastic debris **Banded Iron Formation (BIF)** Oceanic crust: Older metavolcanics	Arc volcanism: Younger (Shadhli metavolcanics) Migmatites	D1: isoclinal folds in amphibolite xenoliths in core complexes
1800 — 850	Migmatites		Migmatites	

Fig. 2: Stratigraphic and lithotectonic units of the Egyptian Eastern Desert related in space and time to the deformational events identified by Loizenbauer et al. (2001) and Shalaby et al. (2005).

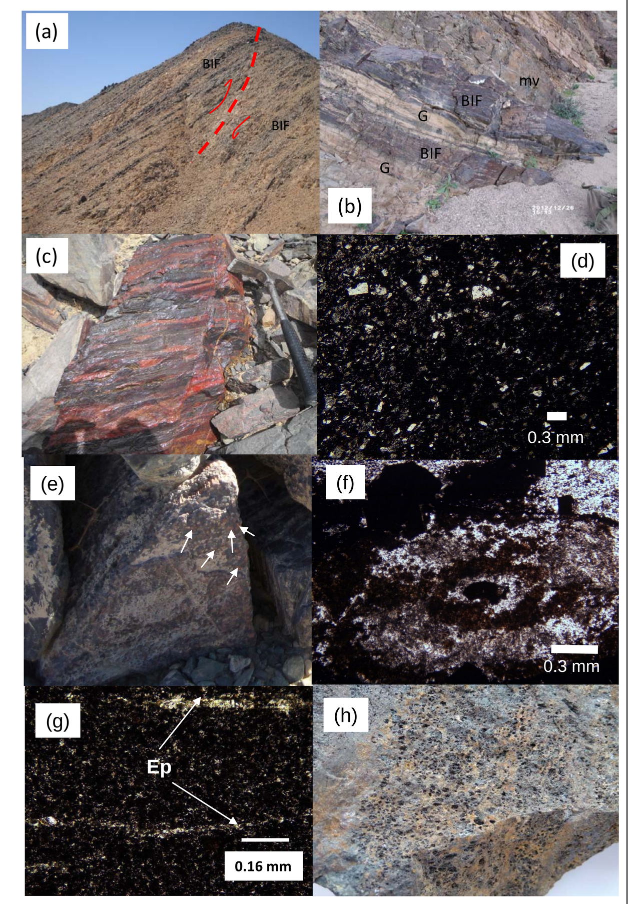

Fig. 3 (a) Folded and faulted BIF intercalated with metavolcaniclastics, Um Nar, looking NW; (b) 20 – 30 cm thick bands of iron ore intercalated with metavolcaniclastics (mv), and intruded by granitic sills (G); El Imra; (c) Continuous and streaky rhythmic banding in BIF (d) Lithic fragments in W. El Dabbah BIF, XPL; (e) Granular BIF with reddish pisolites (arrows); average radius ~ 0.35 cm; Abu Marwat; (f) Photomicrograph of a pisolite, Abu Marwat; concentric layers of quartz with dusty hematite/ ferrihydrite? + goethite/ lepidocrocite + chlorite, PPL; (g) BIF with veins of epidote, XPL; (h) porous texture developed by hydrothermal alteration?, Wadi Kareim.

III-Petrography and mineral chemistry

- Silica rich bands range from jaspilites to quartz-rich bands that include magnetite, hematite, garnet, epidote, and calcite (Fig. 4a) ± actinolite, diopside, plagioclase, chlorite, stilpnomelane, and apatite. Garnet is restricted to Um Nar, El Imra, Um Ghamis, and W. El Dabbah, whereas stilpnomelane ± greenalite are restricted to the northern deposits of Wadi Kareim and Hadrabia.
- Magnetite occurs in three generations: (i) very fine-grained euhedral crystals (Fig. 4b); (ii) medium-grained crystals with sieve textures and/ or patchy to oscillatory zoning (Figs. 4c - e); and (iii) coarser-grained porphyroblasts (Fig. 4g).
- Hematite varieties include (i) fine-grained acicular crystals oriented with the banding; (ii) coarser-grained crystals replacing magnetite II (Fig. 4h); and (iii) coarse- grained specularite in apparent textural equilibrium with magnetite III.
- Lepidocrocite ± goethite are common weathering products.

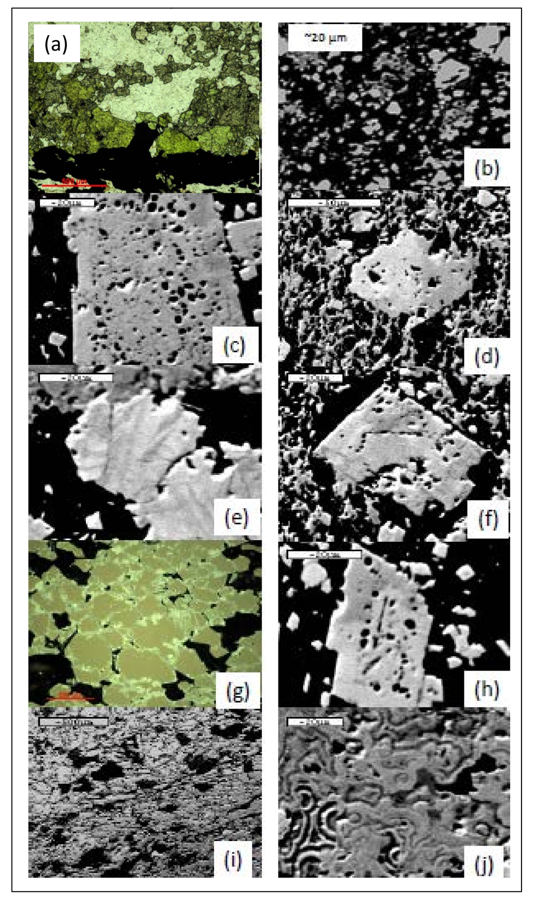

Fig. 4: Photomicrographs of (a) Magnetite and hematite alternating with garnet + epidote, Um Nar; (PPL). (b) BSEI of magnetite I (bright) in quartz (black), with chlorite (grey). (c) BSEI of sieve textured magnetite II with inclusions of quartz. (d) BSEI of partially martitized magnetite II. (e) BSEI of magnetite II with oscillatory zoning. (f) BSEI of magnetite II altered to hematite. (g) Magnetite III partially martitized, Um Nar, (PPL). (h) BSEI of magnetite II pseudomorphed by hematite, W. El Dabbah. (i) BSEI of dense mass of specularite, Um Nar; (j) BSEI of colloform lepidocrocite, W. Kareim.

V- Geochemistry of Host Rocks

(a) Metavolcaniclastic rocks

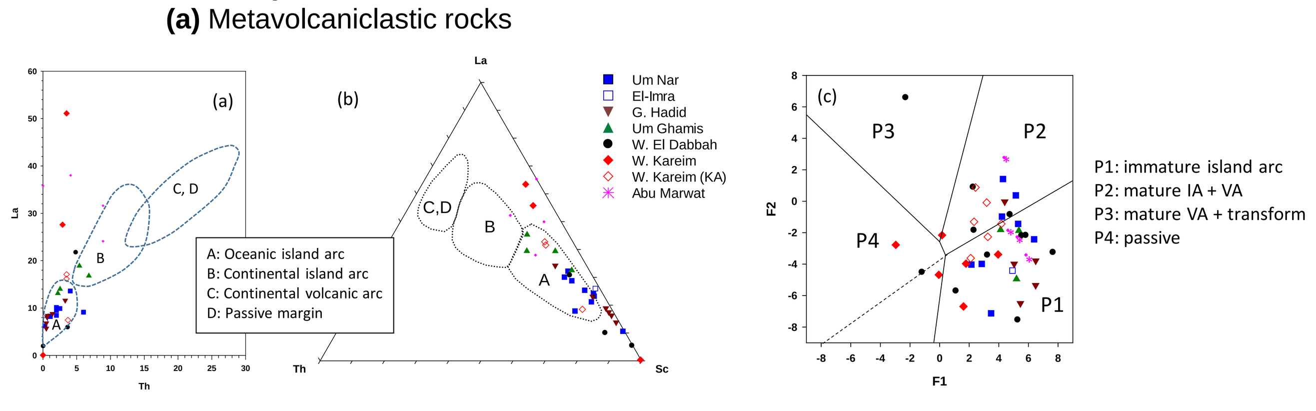

Fig. 9: Discriminant diagrams for metavolcaniclastics. (a) and (b) La vs. Th and La – Th – Sc ternary of Bathia and Crook (1986). (c) Trace element discriminant functions (F1 and F2) and diagram of Roser and Korsch (1988).

IV- Geochemistry of BIF

- CED BIFs have higher Fe^T compared to Algoma or Superior BIFs; However, this Fe enrichment is not related to hydrothermal alteration or weathering (Figs. 5a & b).
- Factor matrix analysis shows three associations: (i) Al, Mg, Ti ± Zr ± Y; (ii) Fe & Si; (iii) Ca, P. $Fe_2O_3^T$ and SiO_2 are positively correlated, defining 3 trends (Fig. 5c).
- Elements indicative of a detrital origin are positively correlated defining 3 trends (Figs. 5d, e).

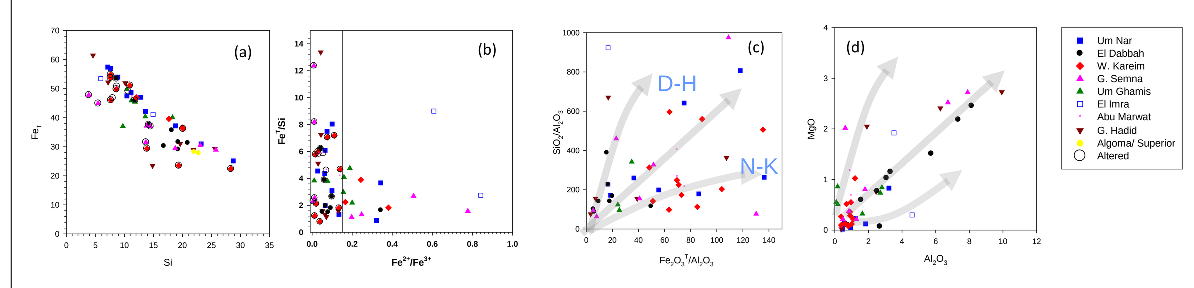

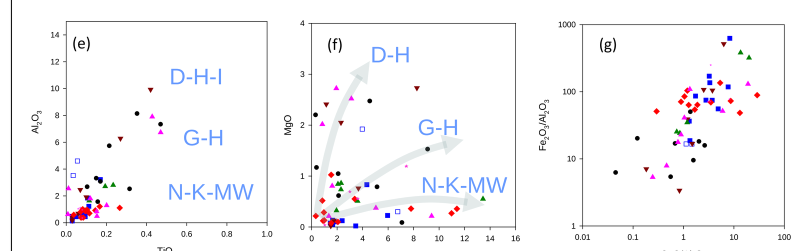

Fig. 5: Geochemical characteristics and correlations for CED BIFs. Arrows suggest possible correlation trends. D: Wadi El Dabbah, H: Gebel El Hadid; N: Um Nar; K: Wadi Kareim; MW: Abu Marwat; I: El Imra.

- Positive correlation between Ca and Mg, and lack of correlation between Ca and Fe among hydrothermally altered samples (Wadi Kareim and Abu Marwat; Figs. 5f & g) indicate that hydrothermal alteration/ Ca-metasomatism did not cause Fe-enrichment of CED BIFs.
- Geochemical trends show that Wadi El Dabbah and El Imra have the highest concentration of elements indicative of a detrital origin, whereas Um Nar has the lowest such concentrations but the highest Y/Ho and lowest Pr/Yb ratios (Figs. 6a - c).

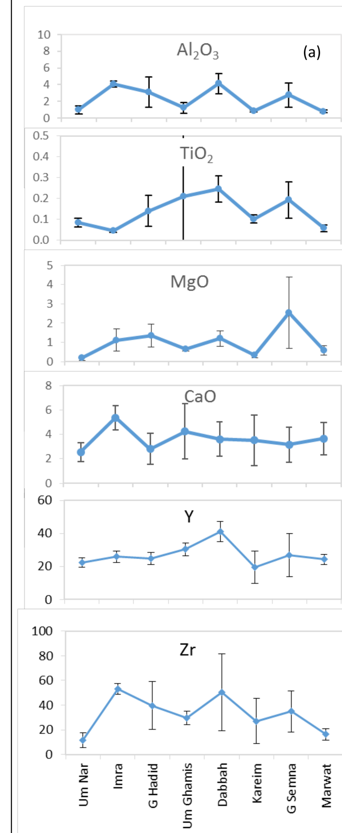

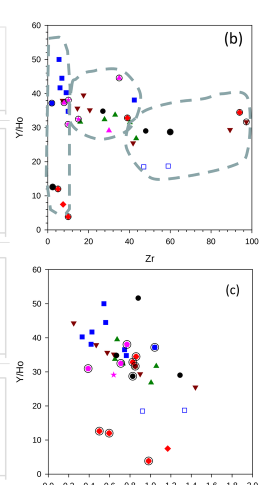

Fig. 6: (a) Geochemical trends for BIFs across the CED; (b) & (c) Y/Ho vs. Zr and Pr/Yb. Plots show W El Dabbah and El Imra with highest detrital input; and Um Nar ± W. Kareim closest to the vents. Symbols as in Fig. 5.

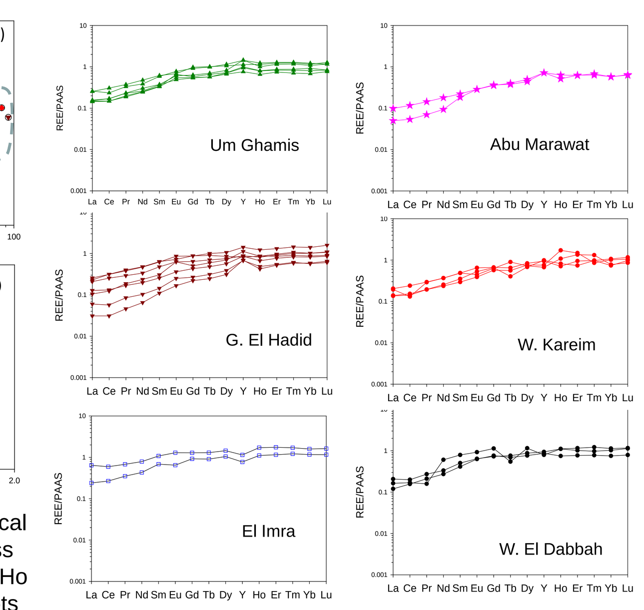

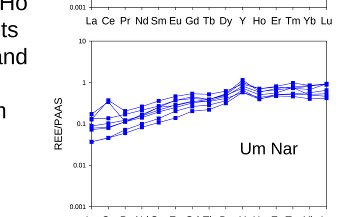

Fig. 7: REE-Y patterns normalized to PAAS for CED BIFs investigated in this study.

- PAAS normalized RE-Y concentrations for all BIFs show LREE enrichment with a few samples displaying a weak + Eu anomaly; this indicates a hydrogeneous origin for these BIFs with some hydrothermal component (Fig. 7).
- A hydrothermally influenced hydrogeneous origin (with a relatively small detrital component) for the CED BIFs is also indicated by plots of Fe/Ti vs. Al/(Al+Fe+Mn), SiO_2 vs. Al_2O_3, and ∑REE vs. Co + Cu + Ni plots of Peters (2003), Wonder et al. (1988), and Klein & Beukes (1993), respectively (Figs. 8 a- c),

(b) Metavolcanic rocks

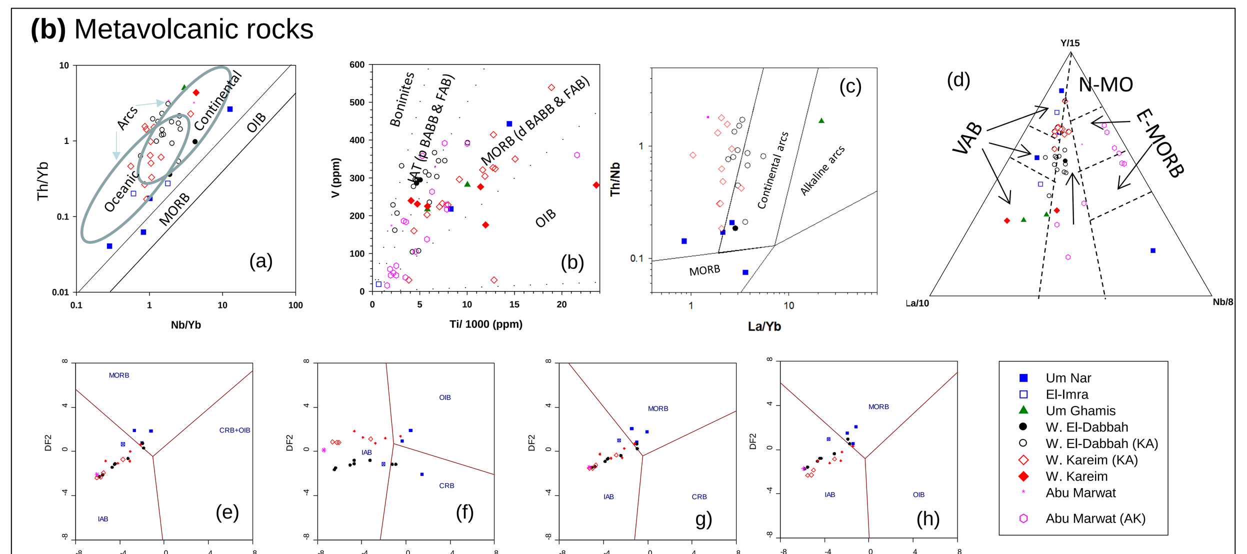

Fig. 10: Chemical characterization of metavolcanic rocks associated with CED BIFs. (a) Th/Yb vs. Nb/Yb diagram of Pearce (2008; 2014). (b) Ti vs. V diagram of Shervais (1982). (c) Th/Nb vs. La/Yb discriminant diagram of Hollocher et al. (2012). (d) Y – La – Nb diagram of Cabanis and Lecolle (1989) for metabasaltic samples. (e) – (h) Trace element discriminant functions (DF1 and DF2) of Agrawal et al. (2008) for metabasaltic samples. KA: data from Ali et al. (2009); AK: data from Mohamed Abdel Kareem (2018; pers. Comm).

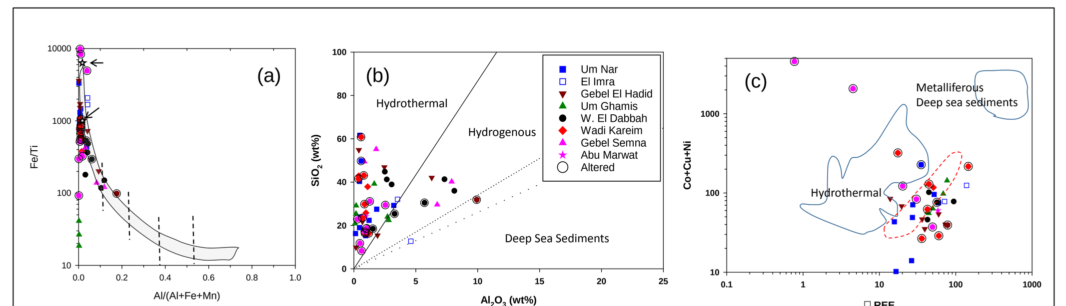

Fig. 8: Chemistry of CED BIFs on diagrams of (a) of Peter (2003), (b) Wonder et al. (1988), and Klein & Beukes (1993).

VI- Tectonic Evolution of the CED and origin of BIFs

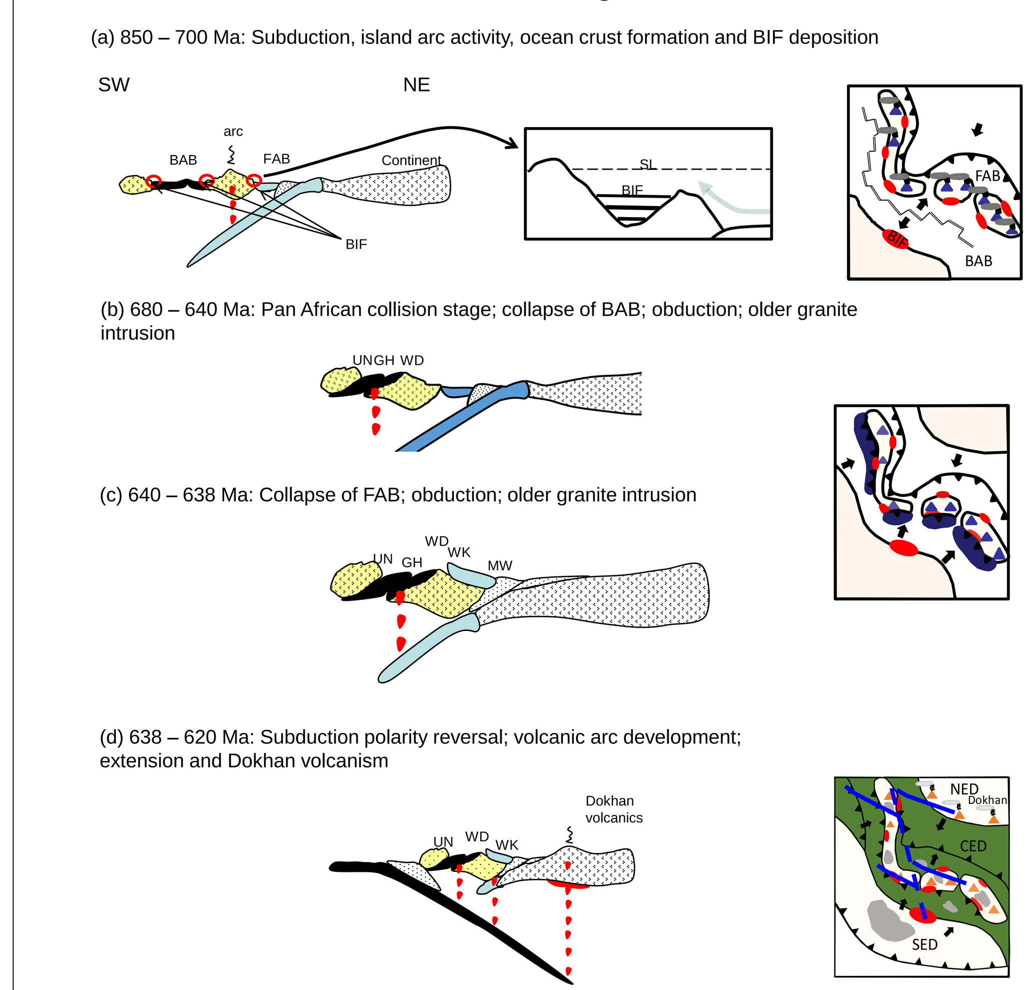

Fig. 11: Proposed tectonic evolution for CED depicted through several cross sectional views all in the NE – SW direction (present day coordinates) and corresponding map views (insets). Red circles/ areas: possible locations for the deposition of BIFs. Inset for Fig. (a) shows the proposed depositional model for BIF in a silled, terraced, fore-arc basin (cf. Dickinson, 1995); SL: sea level; arrow represents upwelling of relatively anoxic waters into the oxygenated silled basin. BAB: back arc basin, FAB: fore arc basin, UN, GH, WD, WK, and MW: relative locations of BIFs of Um Nar, Gebel Hadid, Wadi El Dabbah, Wadi Kareim, and Abu Marwat, respectively.

VII- Conclusions

- All BIFs have a hydrogenous origin influenced by hydrothermal solutions, and received a relatively small amount of detrital material.
- Volcanic and volcaniclastic rocks interlayered with the BIFs have geochemical signatures characteristic of an immature island arc (Fig. 10a & b). Um Nar samples show some MORB affinity. All volcanic rock analyses are compatible with back- and fore-arc basins (Figs. 10c & d).
- Fe and Si were provided by submarine hydrothermal solutions mostly on the floor of small basins adjacent to an active, immature island arc. During periods of arc activity, ash and dust covered these basins depriving their waters from atmospheric O_2 and increasing the concentration of Fe^{2+} in water.
- BIF mineral precursors were precipitated during periods of arc quiescence, triggered by upwelling of Fe^{2+} rich hydrothermal fluids into more oxygenated layers of the small, terraced or sloped, silled basins in the fore- and back-arc areas, or in rift-related intra-arc basins. CED BIFs are non-glaciogenic in origin
- Geochemical trends, Y/Ho, and Pr/Yb ratios suggest that Wadi El Dabbah BIF was deposited closest to the arc, whereas Um Nar, Abu Marwat ± Wadi Kareim formed farthest from it, but closest to the hydrothermal vents.
- Factor analysis shows 4 to 5 main factors the most prominent of which are the positively correlated Al, Mg, Y, ± Zr ± Ti factor representing detrital components, and the Fe and Si ± Cu factor representing the chemical precipitates. Correlation diagrams among the detrital factor elements show three distinct trends, which may reflect three main volcanic pulses at 828 ± 5, 772 ± 5, and 728 ± 4 Ma (El-Shazly & Khalil, 2016).
- Hydrothermal alteration manifested by secondary Ca-rich minerals was localized and may have been related to either serpentinization of ultrabasic bodies, or intrusion of older granitoids. However, the geochemical data presented is insufficient to support either conclusion.
- Weathering increased Fe^{3+}/Fe^{2+} ratios of BIFs, generally leached silica, and increased some of their trace element concentrations.
- The geochemical data provided for the two samples from El Imra, which suggest an intra-arc origin, are relatively enigmatic (very high Ca, Al, Y, V, Sc, La, and Ce) compared to the other BIFs. More work on a larger number of samples from this area is therefore needed.